

Atmospheric Chemistry of Two Biodiesel Model Compounds: Methyl Propionate and Ethyl Acetate

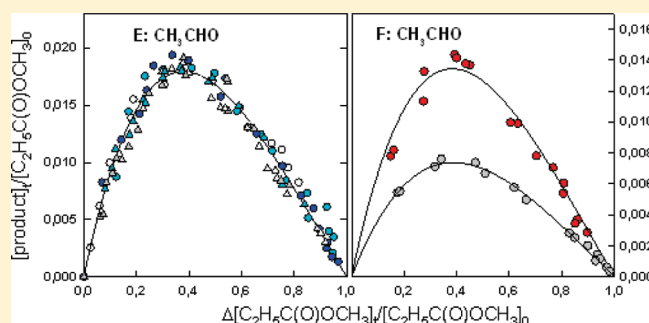
Vibeke F. Andersen,[†] Tesfaye A. Berhanu,[†] Elna J. K. Nilsson,[†] Solvejg Jørgensen,[†] Ole John Nielsen,[†] Timothy J. Wallington,[‡] and Matthew S. Johnson^{*,†}

[†]Copenhagen Center for Atmospheric Research (CCAR), Department of Chemistry, University of Copenhagen, Universitetsparken 5, 2100 København Ø, Denmark

[‡]Systems Analytics and Environmental Sciences Department, Research and Advanced Engineering, Ford Motor Company, Mail Drop RIC-2122, Dearborn, Michigan 48121-2053, United States

Supporting Information

ABSTRACT: The atmospheric chemistry of two $C_4H_8O_2$ isomers (methyl propionate and ethyl acetate) was investigated. With relative rate techniques in 980 mbar of air at 293 K the following rate constants were determined: $k(C_2H_5C(O)OCH_3 + Cl) = (1.57 \pm 0.23) \times 10^{-11}$, $k(C_2H_5C(O)OCH_3 + OH) = (9.25 \pm 1.27) \times 10^{-13}$, $k(CH_3C(O)OC_2H_5 + Cl) = (1.76 \pm 0.22) \times 10^{-11}$, and $k(CH_3C(O)OC_2H_5 + OH) = (1.54 \pm 0.22) \times 10^{-12} \text{ cm}^3 \text{ molecule}^{-1} \text{ s}^{-1}$. The chlorine atom initiated oxidation of methyl propionate in 930 mbar of N_2/O_2 diluent (with, and without, NO_x) gave methyl pyruvate, propionic acid, acetaldehyde, formic acid, and formaldehyde as products. In experiments conducted in N_2 diluent the formation of $CH_3CHClC(O)OCH_3$ and $CH_3CCl_2C(O)OCH_3$ was observed. From the observed product yields we conclude that the branching ratios for reaction of chlorine atoms with the CH_3- , $-CH_2-$, and $-OCH_3$ groups are $<49 \pm 9\%$, $42 \pm 7\%$, and $>9 \pm 2\%$, respectively. The chlorine atom initiated oxidation of ethyl acetate in N_2/O_2 diluent gave acetic acid, acetic acid anhydride, acetic formic anhydride, formaldehyde, and, in the presence of NO_x , PAN. From the yield of these products we conclude that at least $41 \pm 6\%$ of the reaction of chlorine atoms with ethyl acetate occurs at the $-CH_2-$ group. The rate constants and branching ratios for reactions of OH radicals with methyl propionate and ethyl acetate were investigated theoretically using transition state theory. The stationary points along the oxidation pathways were optimized at the CCSD(T)/cc-pVTZ//BHandHLYP/aug-cc-pVTZ level of theory. The reaction of OH radicals with ethyl acetate was computed to occur essentially exclusively ($\sim 99\%$) at the $-CH_2-$ group. In contrast, both methyl groups and the $-CH_2-$ group contribute appreciably in the reaction of OH with methyl propionate. Decomposition via the α -ester rearrangement (to give $C_2H_5C(O)OH$ and a HCO radical) and reaction with O_2 (to give $CH_3CH_2C(O)OC(O)H$) are competing atmospheric fates of the alkoxy radical $CH_3CH_2C(O)OCH_2O$. Chemical activation of $CH_3CH_2C(O)OCH_2O$ radicals formed in the reaction of the corresponding peroxy radical with NO favors the α -ester rearrangement.



1. INTRODUCTION

Concerns related to climate change and energy security combined with a desire to provide support for rural communities has led to a substantial increase in the global production of biofuels over the past decade. Ethanol produced from corn and sugar cane is the dominant biofuel in the US and in Brazil, respectively, and is typically blended into gasoline before use (e.g., in E10, E25, E85). Fatty acid methyl esters (FAMES) made from transesterification of plant oils or animal fats are the dominant biofuel in the EU and are typically blended into petroleum diesel before use (e.g., in B2, B20). FAME is usually also referred to as “biodiesel” as distinct from hydrotreated vegetable oils which are referred to as “renewable diesel”. The

majority of global biodiesel is produced in Europe, with rapeseed and sunflower being the two major feedstocks.^{1–3}

The widespread use of FAMES in diesel blends will lead to their release into the atmosphere. The atmospheric oxidation of esters is initiated by reaction with OH radicals and, to a lesser extent, chlorine atoms. Detailed kinetic and mechanistic data concerning these reactions are needed as inputs for atmospheric chemistry models to assess the environmental impacts associated with release of esters into the air. The available database concerning the atmospheric chemistry of esters is

Received: May 24, 2011

Revised: July 9, 2011

Published: July 11, 2011

Table 1. Rate Constants (Units of $10^{-12} \text{ cm}^3 \text{ molecule}^{-1} \text{ s}^{-1}$) for Reactions of Chlorine Atoms and OH Radicals with Methyl Propionate and Ethyl Acetate

reaction	<i>k</i>	method	reference
(1) $\text{C}_2\text{H}_5\text{C}(\text{O})\text{OCH}_3 + \text{Cl} \rightarrow \text{products}$	15.7 ± 2.3	relative rate 293 \pm 0.5 K, 980 mbar air	this study
	19.8 ± 2.6	absolute rate 298 \pm 2 K, 19.5–78 mbar He	Notario et al. ⁶
	15.1 ± 2.2	relative rate 296 \pm 2 K, 990 mbar air	Cavalli et al. ⁷
(2) $\text{C}_2\text{H}_5\text{C}(\text{O})\text{OCH}_3 + \text{OH} \rightarrow \text{products}$	0.925 ± 0.127	relative rate 293 \pm 0.5 K, 980 mbar air	this study
	0.38	ab initio ^a Transition state theory, 298 K	this study
	0.929 ± 0.113	relative rate 296 K, 990 mbar air	Cavalli et al. ⁷
	1.03 ± 0.04	absolute rate 296 K, 33–70 mbar Ar	Wallington et al. ⁸
	0.83 ± 0.09	absolute rate 298 K, 133 mbar He	Le Calvé et al. ⁹
(3) $\text{CH}_3\text{CHClC}(\text{O})\text{OCH}_3 + \text{Cl} \rightarrow \text{products}$	2.71 ± 0.39	relative rate 293 \pm 0.5 K, 980 mbar N_2	this study
(4) $\text{CH}_3\text{C}(\text{O})\text{OC}_2\text{H}_5 + \text{Cl} \rightarrow \text{products}$	17.6 ± 2.2	relative rate 293 \pm 0.5 K, 980 mbar air	this study
	20.1 ± 2.5	absolute rate 298 \pm 2 K, 20–80 mbar air	Notario et al. ⁶
	13.7 ± 2.0	absolute rate 264.5–380 K, 26–270 mbar He	Cuevas et al. ¹⁰
	17.6 ± 1.1	absolute rate 298 \pm 2 K, 3–930 mbar N_2	Xing et al. ¹¹
	17.6 ± 2.6	relative rate 296 \pm 1 K, 3–933 mbar N_2	Xing et al. ¹¹
(5) $\text{CH}_3\text{C}(\text{O})\text{OC}_2\text{H}_5 + \text{OH} \rightarrow \text{products}$	1.54 ± 0.22	relative rate 293 \pm 0.5 K, 980 mbar air	this study
	2.00	ab initio ^a transition state theory, 298 K	this study
	1.51 ± 0.14	absolute rate 296 K, 33–70 mbar Ar	Wallington et al. ⁸
	1.67 ± 0.22	absolute rate 298 K, 1133 mbar He	El Boudali et al. ¹³
	1.73 ± 0.20	relative rate 298 \pm 4 K, 1013 mbar air	Picquet-Varrault et al. ¹⁴

^aCCSD(T)/cc-pVTZ//BHandHLYP/aug-cc-pVTZ.

limited,^{4,5} and the present work was undertaken to improve our understanding of the chemistry of this class of oxygenated organic compound.

The FAMES present in biodiesel (e.g., methyl oleate, methyl linoleate) have low vapor pressures and are difficult to study in smog chamber systems. In the present study we investigate, using experimental and computational methods, the chemistry of two small esters as models for the larger esters present in biodiesel. We conducted an experimental investigation of the kinetics and products of the OH radical and chlorine atom initiated oxidation of methyl propionate and ethyl acetate in 930–980 mbar of N_2/O_2 diluent with, and without, added NO at 293–296 K. In addition we conducted a computational study of the kinetics of reactions of OH radicals with methyl propionate and ethyl acetate.

Two previous studies of $k(\text{Cl} + \text{methyl propionate})$ ^{6,7} and three studies of $k(\text{OH} + \text{methyl propionate})$ ^{7–9} have been reported. A study of the chlorine atom initiated oxidation of methyl propionate in 740 Torr air, at 296 K in the presence of NO was performed by Cavalli et al.⁷ There are no reported studies of the oxygen and NO dependence of the oxidation mechanism of methyl propionate. No theoretical studies of the OH-initiated oxidation of methyl propionate have been reported. Three previous studies of $k(\text{Cl} + \text{ethyl acetate})$ ^{6,10,11} and three studies of $k(\text{OH} + \text{ethyl acetate})$ ^{8,12,13} have been reported. The previous kinetic studies are summarized in Table 1. The products of the OH radical initiated oxidation of ethyl acetate in air at ambient temperature and pressure in the presence of NO have been studied by Tuazon et al.¹⁴ and Picquet-Varrault et al.¹⁵ The oxygen and temperature dependence of the products of chlorine initiated oxidation of ethyl acetate have been described by Orlando and Tyndall.¹⁶ The present work is the first experimental study of the NO_x dependence of the product branching ratios of the chlorine atom initiated oxidation of ethyl acetate and the first theoretical study of the kinetics of the reactions of OH radicals with ethyl acetate.

2. EXPERIMENTAL SETUP

Experiments were performed in the photochemical reactors at CCAR in Copenhagen¹⁷ and at Ford Motor Company in Dearborn, MI.¹⁸ The system in Copenhagen consists of a 100-L quartz reaction chamber sealed at both ends with stainless steel flanges and surrounded by 8 UV-A (325–380 nm), 16 UV-C (254 nm), and 12 broad band sun lamps (325 nm to infrared). The system is enclosed in an insulating box equipped with a temperature control system to ensure stable (within 0.5 K) temperatures during experiments. Gas mixtures in the chamber were monitored with a Bruker IFS 66v/s FTIR spectrometer using an IR path length of 72 m and resolution of 0.125 cm^{-1} .

The system at Ford Motor Company consists of a 140-L Pyrex reactor interfaced to a Mattson Sirius 100 FTIR spectrometer. The reactor is surrounded by 22 fluorescent blacklamps (GE F40T12BLB) which were used to initiate the experiments. Concentrations of reactants and products were monitored by FTIR spectroscopy. IR spectra were derived from 32 coadded interferograms with a spectral resolution of 0.25 cm^{-1} and an analytical path length of 27.1 m. The experiments were performed at $296 \pm 2 \text{ K}$.

3. MATERIALS AND METHOD

Relative rate methods were used to measure rate constants for the following reactions

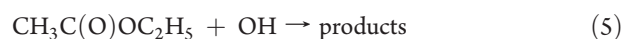
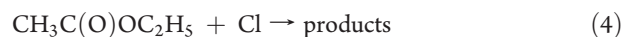
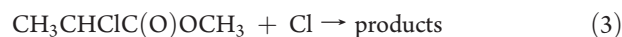
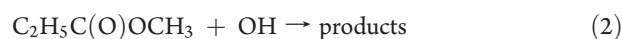
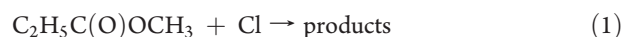


Table 2. Reference Rate Constants Used in This Work

reaction	rate constant (cm ³ molecule ⁻¹ s ⁻¹)	reference
(6) C ₂ H ₅ Cl + Cl → products	8.04 × 10 ⁻¹²	37
(7) C ₂ H ₄ + Cl → products	9.29 × 10 ⁻¹¹	38
(8) C ₂ H ₆ + Cl → products	5.9 × 10 ⁻¹¹	39
(9) C ₃ H ₈ + Cl → products	1.40 × 10 ⁻¹⁰	39
(10) C ₂ H ₆ + OH → products	2.40 × 10 ⁻¹³	39
(11) <i>c</i> -C ₆ H ₁₂ + OH → products	6.37 × 10 ⁻¹²	40
(12) C ₃ H ₈ + OH → products	1.10 × 10 ⁻¹²	39

Reactions 6–12 were employed as the reference reactions. The reference rate constants used are listed in Table 2.



k_1 was determined relative to k_6 and k_7 , k_2 was determined relative to k_{10} and k_{11} , k_3 was determined relative to k_6 and k_8 , k_4 was determined relative to k_6 , k_7 , and k_9 , and k_5 was determined relative to k_{11} and k_{12} . All chemicals were obtained from commercial sources: C₂H₅C(O)OCH₃ (≥99.0%, Fluka), CH₃CHClC(O)OCH₃ (97%, Aldrich), CH₃C(O)OC₂H₅ (99.8%, Sigma-Aldrich), C₂H₅Cl (≥99.7%, Gerling Holz + CO), C₂H₆ (≥99.95%, Fluka), C₂H₄ (≥99.5%, Aldrich), *c*-C₆H₁₂ (99.5%, Aldrich), and C₃H₈ (98%, Aldrich).

Relative rate experiments were performed in 980 mbar of air, or N₂, diluent. Product studies were performed in 930 mbar of N₂/O₂ diluent with O₂ partial pressures of 70–930 mbar in the presence and absence of NO. The photochemical chain chlorination of methyl propionate was studied in 980 mbar of N₂ diluent. Experimental conditions are shown in Tables S1 and S2 in the Supporting Information. Chlorine atoms were generated by photolysis of Cl₂ in mixtures containing methyl propionate or ethyl acetate and reference compounds. OH radicals were generated by the photolysis of O₃ in the presence of H₂O. O₃ was generated from O₂ with an ozone generator from O₃ Technology and condensed on silica gel that was cooled with ethanol and dry ice to approximately -70 °C. The initial concentration of ozone and water vapor was approximately 5 times the total concentration of reactants. Photolysis intervals were typically between 5 s and 10 min, and an IR spectrum was recorded after each photolysis step.

The IR absorption spectra of methyl propionate and ethyl acetate are provided in the Supporting Information. The reaction rates were determined using the relative rate method. Assuming that the reactant and reference compounds are only lost via the reaction of interest and that neither the reactant nor the reference

is formed in the system, the following relation is valid

$$\ln\left(\frac{[\text{reference}]_0}{[\text{reference}]_t}\right) = \frac{k_{\text{reference}}}{k_{\text{reactant}}}\ln\left(\frac{[\text{reactant}]_0}{[\text{reactant}]_t}\right) \quad (I)$$

where [reactant]₀ and [reference]₀ are the initial concentrations of reactant and reference, respectively, and [reactant]_t and [reference]_t are the concentrations of reactant and reference at time *t*. Plotting the loss of reactant versus reference compound gives a straight line with slope $k_{\text{reactant}}/k_{\text{reference}}$. Unless stated otherwise, all quoted uncertainties are 2 standard deviations from least-squares regressions and include uncertainties in the analysis of the IR spectra (typically 5–10%).

4. COMPUTATIONAL DETAILS

The methodology used in the present work was the same as that employed in our recent study of the reaction of OH radicals with methyl acetate.¹⁹ The geometries of the stationary points along the reaction path were optimized using density functional theory BHandHLYP^{20,21} with the basis set aug-cc-pVTZ.²² The calculated frequencies were used to characterize the stationary points (a minimum or a saddle point) and to estimate the zero point vibrational energy (ZPE). A single point energy optimization with the coupled cluster single and double excitation method including a perturbative estimate of triples (CCSD(T))²³ and the cc-pVTZ basis set was used to obtain reliable energies at each stationary point. All calculations were performed using Gaussian 03.²⁴ One problem with applying unrestricted calculations to these systems is the potential for spin contamination from higher lying spin states. The expectation value of the total spin was less than 0.78 before and 0.75 after spin annihilation. Therefore, spin contamination is not considered to be severe. In general, spin contamination for the transition state structures and the product complexes was larger than that for the reactant complexes.

We observe prereaction complexes with lower energy than the separated reactants. If we assume a fast equilibrium between the reactant and the prereactive complex, we can calculate the rate constant at 298 K using standard transition state theory (TST)²⁵

$$k = \kappa(T)\sigma\frac{k_{\text{b}}T}{h}\left(\frac{Q_{\text{TS}}}{Q_{\text{R}}Q_{\text{OH}}}\right)\exp\left(-\frac{E_{\text{a}}}{k_{\text{b}}T}\right) \quad (II)$$

where $\kappa(T)$ is the quantum tunneling coefficient, σ the symmetry factor, i.e., the number of identical reaction paths, k_{b} Boltzmann's constant, h Planck's constant, T temperature, Q the total partition function, and finally E_{a} is the activation energy at 0 K calculated as $E_{\text{a}} = E_{\text{TS}} - (E_{\text{R}} + E_{\text{OH}})$. The quantum tunneling coefficient was considered using the one-dimensional Wigner transmission coefficient²⁶

$$\kappa(T) = 1 + \frac{1}{24}\left(\frac{h\nu^{\ddagger}}{k_{\text{b}}T}\right)^2 \quad (III)$$

where ν^{\ddagger} is the imaginary frequency associated with the reaction coordinate.

5. RELATIVE RATE RESULTS

To test for photolysis, mixtures containing methyl propionate, ethyl acetate and the reference compounds (but not Cl₂ or O₃/H₂O) in air were irradiated using conditions (number of lamps and time span) similar to those used in the relative rate experiments. To test for

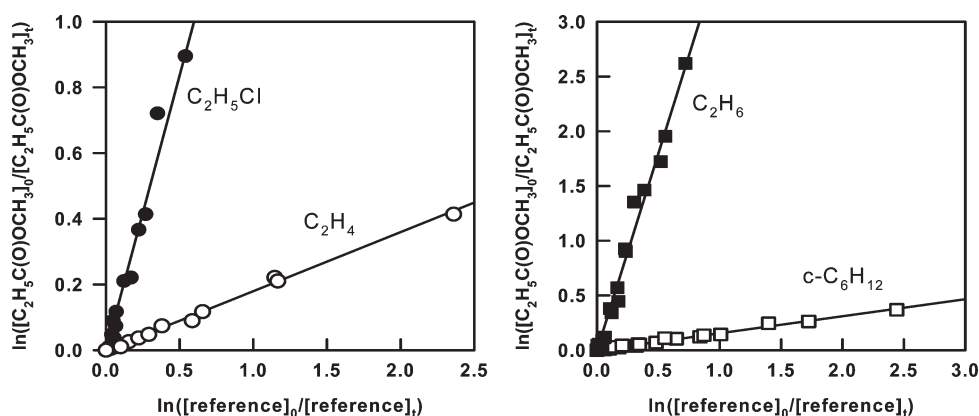


Figure 1. Relative rate plots for the reaction of methyl propionate with Cl (left) and OH (right) in 980 mbar air at 293 ± 0.5 K.

Table 3. Results for Relative Rate Studies of the Cl and OH Initiated Oxidations of Methyl Propionate, Methyl-2-chloropropionate and Ethyl Acetate^a

reaction	$k_{\text{ester}}/k_{\text{reference}}$	rate constant ($\times 10^{12}$ $\text{cm}^3 \text{ molecule}^{-1} \text{ s}^{-1}$)
(1) relative to (6)	1.81 ± 0.43	14.6 ± 3.4
(1) relative to (7)	0.18 ± 0.03	16.7 ± 3.1
(2) relative to (10)	3.65 ± 0.72	0.876 ± 0.174
(2) relative to (11)	0.15 ± 0.03	0.974 ± 0.185
(3) relative to (6)	0.328 ± 0.064	2.64 ± 0.52
(3) relative to (8)	0.047 ± 0.010	2.78 ± 0.59
(4) relative to (6)	1.93 ± 0.38	15.5 ± 3.1
(4) relative to (7)	0.184 ± 0.036	17.1 ± 3.3
(4) relative to (9)	0.145 ± 0.033	20.3 ± 4.6
(5) relative to (11)	0.234 ± 0.044	1.49 ± 0.28
(5) relative to (12)	1.43 ± 0.30	1.58 ± 0.33

^aExperiments were performed at 293 ± 0.5 K.

unwanted heterogeneous reactions, mixtures (including Cl_2 or $\text{O}_3/\text{H}_2\text{O}$) were left for 10–30 min in the chamber in the dark. There was no discernible loss (<1%) of the reactants in these control experiments.

5.1. Methyl Propionate. *Cl Experiments.* $\text{C}_2\text{H}_5\text{Cl}$ and C_2H_4 were used as reference compounds in the study of the reaction of chlorine atoms with methyl propionate. $\text{C}_2\text{H}_5\text{Cl}$ was monitored using its absorption peak at 1289 cm^{-1} . The absorption peak due to $\text{C}=\text{O}$ stretching at $1720\text{--}1800 \text{ cm}^{-1}$ was used to follow methyl propionate and the absorption overtone peak at 1889 cm^{-1} from the $\text{C}\text{--}\text{H}$ out-of-plane torsion was used for C_2H_4 . Relative rate plots are shown in Figure 1. Results from the linear least-squares analyses of the data in Figure 1 are provided in Table 3. The results obtained using the two reference compounds are in agreement within the experimental uncertainties. We cite a final value of $k_1 = (1.57 \pm 0.23) \times 10^{-11} \text{ cm}^3 \text{ molecule}^{-1} \text{ s}^{-1}$ which is the average of the individual determinations with error limits from the weighted average of the determinations. As seen from Table 1, our result is in good agreement with that reported by Cavalli et al.⁷ but is approximately 20% lower than that reported by Notario et al.⁶ (see Table 1). What appears to be a small, but discernible, systematic overestimation of some of the rate constants reported by Notario et al.⁶ has been noted and discussed previously.^{7,11}

OH Experiments. C_2H_6 and $c\text{-C}_6\text{H}_{12}$ were used as reference compounds in the study of the reaction of OH radicals with methyl propionate. The absorption peaks from the $\text{C}\text{--}\text{H}$ stretching vibrations at 2895 and 2865 cm^{-1} were used to monitor C_2H_6 and $c\text{-C}_6\text{H}_{12}$, respectively. The relative rate plots are shown in Figure 1, and results from the linear least-squares analyses are provided in Table 3. The results obtained using the two reference compounds agree within the experimental uncertainties. We cite a final value of $k_2 = (9.25 \pm 1.27) \times 10^{-13} \text{ cm}^3 \text{ molecule}^{-1} \text{ s}^{-1}$ which is an average of the individual determinations with error limits from a weighted average of the determinations. As seen from Table 1, there is good agreement in the results reported in the four experimental studies of the kinetics of the reaction of OH radicals with methyl propionate.

5.2. Methyl-2-chloropropionate. *Cl Experiments.* $\text{C}_2\text{H}_5\text{Cl}$ and C_2H_6 were used as reference compounds for the reaction of methyl-2-chloropropionate with atomic chlorine. The absorption peak due to $\text{C}=\text{O}$ stretching at $1720\text{--}1850 \text{ cm}^{-1}$ was used to follow the methyl-2-chloropropionate concentration. Relative rate plots for the reaction of chlorine atoms with methyl-2-chloropropionate are shown in Figure 2. The rate constants obtained using the two reference compounds agree to within the error limits. We cite a final value of $k_3 = (2.71 \pm 0.39) \times 10^{-12} \text{ cm}^3 \text{ molecule}^{-1} \text{ s}^{-1}$ which is the average of the individual determinations together with error limits which are the weighted average of the determinations. This is the first study of this reaction.

5.3. Ethyl Acetate. *Cl Experiments.* $\text{C}_2\text{H}_5\text{Cl}$, C_2H_4 , and C_3H_8 were used as reference compounds in the study of the reaction of chlorine atoms with ethyl acetate. The absorption peak due to the $\text{C}=\text{O}$ stretching vibration at $1720\text{--}1800 \text{ cm}^{-1}$ was used to determine the ethyl acetate concentration, and the absorption peak at 2968 cm^{-1} from the $\text{C}\text{--}\text{H}$ stretch was used for C_3H_8 . Results of the linear least-squares analyses of the data in Figure 3 are provided in Table 3. The rate constants obtained using the three reference compounds agree to within the error limits. We cite a final value of $k_4 = (1.76 \pm 0.22) \times 10^{-11} \text{ cm}^3 \text{ molecule}^{-1} \text{ s}^{-1}$, which is the average of the individual determinations together with error limits that is the weighted average of the determinations. This value is in agreement, within the combined experimental uncertainties, with the results from previous studies of Xing et al.,¹¹ Notario et al.,⁶ and Cuevas et al.¹⁰

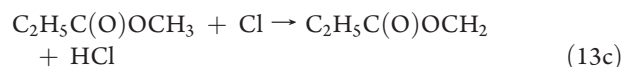
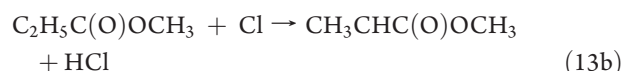
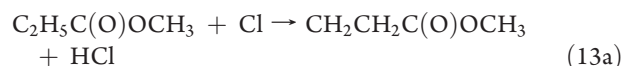
OH Experiments. $c\text{-C}_6\text{H}_{12}$ and C_3H_8 were used as reference compounds in the study of the reaction of OH radicals with ethyl

acetate. The relative rate plots are shown in Figure 3, and the results of the linear least-squares analysis are provided in Table 3. The rate constants obtained using the two reference compounds agree to within the error limits. We cite a final value that is the average of the individual determinations together with error limits that is the weighted average of the determinations, $k_5 = (1.54 \pm 0.22) \times 10^{-12} \text{ cm}^3 \text{ molecule}^{-1} \text{ s}^{-1}$. As seen from Table 1, the result from the present study and those from the previous studies of Wallington et al.,⁸ El Boudali et al.,¹² and Picquet-Varrault et al.¹³ are consistent.

6. PRODUCT STUDIES

6.1. Methyl Propionate. The chlorine atom initiated oxidation of methyl propionate was studied using oxygen partial pressures of 0–930 mbar, in the presence and absence of NO. Experiments in the absence of oxygen were performed at 980 mbar total pressure, all other experiments were performed in 930 mbar total pressure. The oxidation mechanism for methyl propionate is illustrated in Figure 4. Chlorine atom initiated oxidation proceeds via H-abstraction giving three

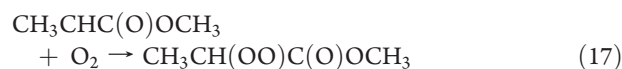
different radicals (reactions 13a–13c).



The chlorinated products $\text{CH}_3\text{CHClC}(\text{O})\text{OCH}_3$ and $\text{CH}_3\text{CCl}_2\text{C}(\text{O})\text{OCH}_3$ were observed in experiments conducted in N_2 diluent. The monochlorinated compound is formed in reaction 14 and further chlorination via reactions 3a and 15 gives the dichlorinated compound. Similar reactions in the chlorination of methyl acetate have been reported previously.^{27,28}



In the presence of oxygen, peroxy radicals are formed from the radicals generated by the H-abstraction reactions.



The peroxy radicals are converted into alkoxy radicals via self-reaction or reaction with NO as illustrated below by reactions 19 and 20 for the peroxy radical formed by reaction 17, and reactions

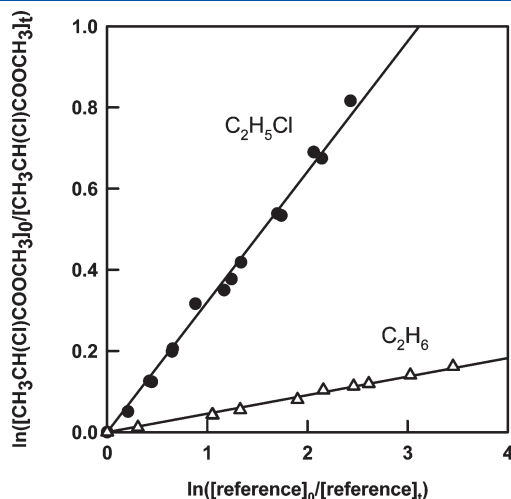


Figure 2. Relative rate plot for the reaction of $\text{CH}_3\text{CH}(\text{Cl})\text{C}(\text{O})\text{OCH}_3$ with Cl in 980 mbar N_2 at $293 \pm 0.5 \text{ K}$.

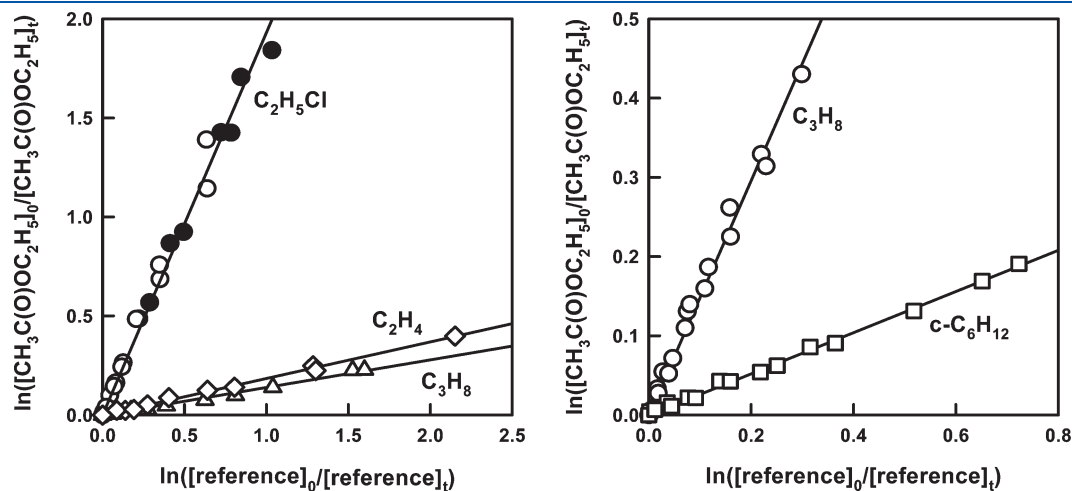


Figure 3. Relative rate plots for the reaction of ethyl acetate with Cl (left) and OH (right) in 980 mbar air (open symbols) or N_2 (closed symbols) at $293 \pm 0.5 \text{ K}$.

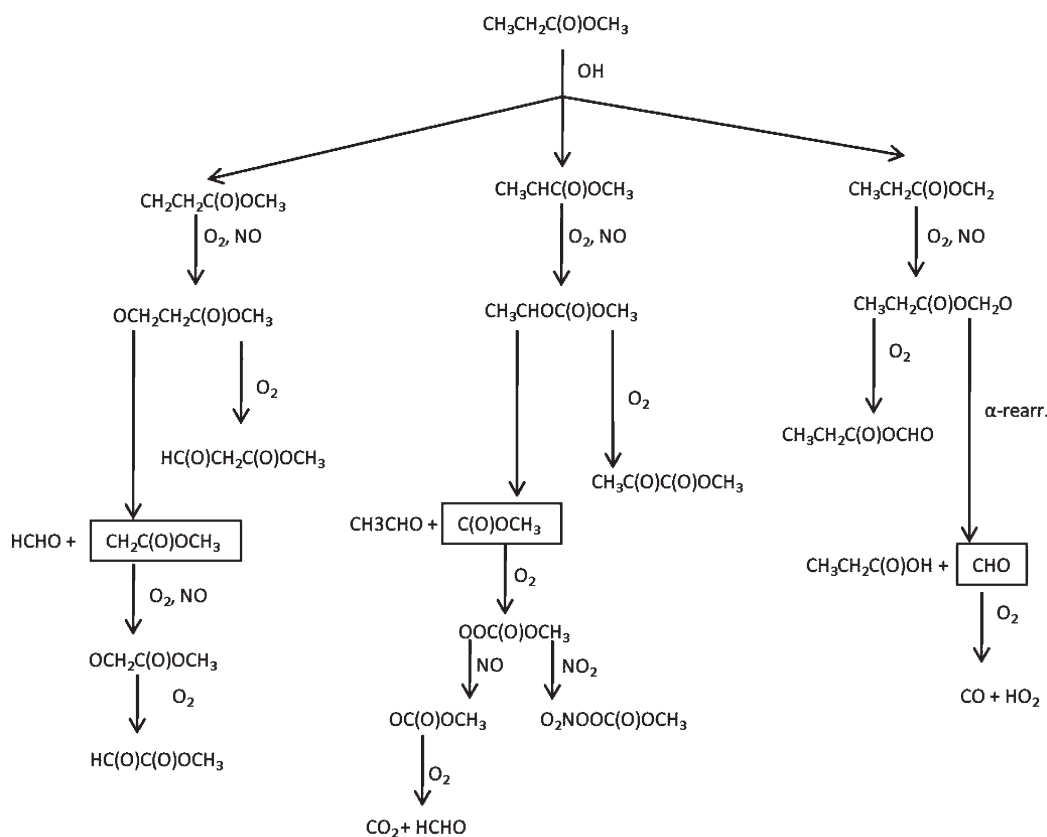
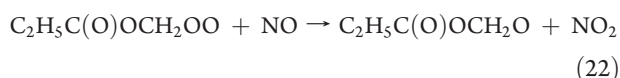
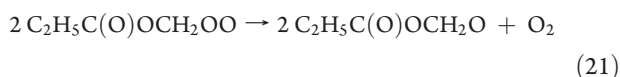
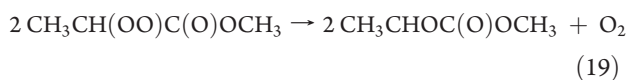


Figure 4. Methyl propionate oxidation mechanism.⁷ The boxes indicate species which undergo further reactions.

21 and 22 for the peroxy radical generated in reaction 18.

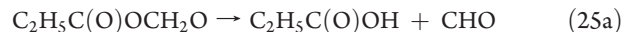


In addition to the alkoxy radicals shown in reactions 20 and 22, organic nitrates can also be formed in the reaction of NO with the peroxy radicals.

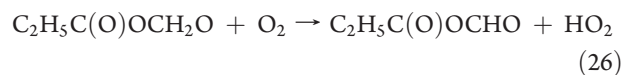
As shown in Figure 4, acids, aldehydes, oxo esters, and anhydrides are formed from subsequent reactions of the alkoxy radicals.

Figure 5 shows spectra derived in an experiment using 200 mbar partial pressure of O₂ in the absence of NO. Panel A shows the spectrum acquired after 75 s of irradiation. Panel B shows the result of subtracting features attributable to methyl propionate from panel A. Comparison of panel B with the reference spectrum in panel C shows the formation of methyl pyruvate. Acetaldehyde, propionic acid, trace amounts of formaldehyde, formic acid, and CO were also identified as products from their characteristic IR features. The alkoxy radical generated in reaction 19 undergoes either decomposition (to give acetaldehyde)

or reaction with O₂ (to give methyl pyruvate) as indicated in reactions 23 and 24. Propionic acid is formed by α-ester rearrangement of C₂H₅C(O)OCH₂O (reaction 25a).



After subtraction of known products absorption peaks were observed at 1040, 1145–1150, 1300, and 1745 cm⁻¹ in the residual spectrum. By comparison with the IR spectrum of acetic formic anhydride²⁹ we assign these features to propionic formic anhydride formed in reaction 26.



Formic acid is formed following the addition of HO₂ radicals to formaldehyde.³⁰



In experiments conducted in the presence of NO, product absorption peaks were observed at 1235, 1306, and 1835 cm⁻¹ which may reflect the formation of methoxy formylperoxynitrate (see Table 2 in Christensen et al.³¹).

The observed products are plotted versus the loss of methyl propionate in Figure 6. In all experiments the concentrations of

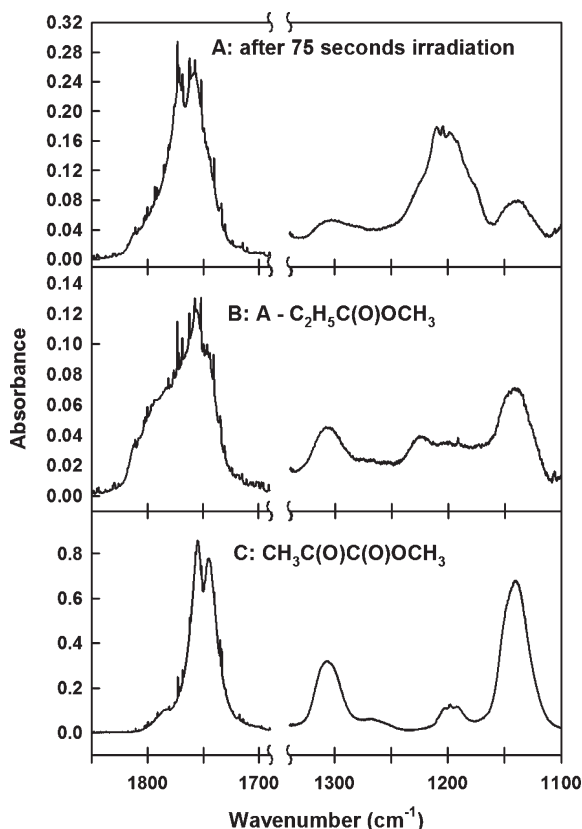


Figure 5. IR spectra acquired after a 75 s UV irradiation of a methylpropionate/ Cl_2 mixture in 930 mbar of air (A) and after subtracting features attributable to methyl propionate (B). Comparison of panel B with the reference spectrum of $\text{CH}_3\text{C}(\text{O})\text{C}(\text{O})\text{OCH}_3$ in panel C shows the formation of this product.

$\text{CH}_3\text{CHClC}(\text{O})\text{OCH}_3$ (for experiments conducted in N_2), $\text{C}_2\text{H}_5\text{C}(\text{O})\text{OH}$, $\text{CH}_3\text{C}(\text{O})\text{C}(\text{O})\text{OCH}_3$, and CH_3CHO initially increased linearly with the loss of methyl propionate. For large consumptions of methyl propionate the loss of products via reaction with chlorine atoms causes the product concentrations to plateau and then decrease with increasing loss of methyl propionate. The shapes of the plots in Figure 6 provide information on the reactivity of the products toward chlorine atoms. The following equation developed by Meagher et al.³² was fitted to the data

$$\frac{[\text{product}]_t}{[\text{CH}_3\text{C}(\text{O})\text{OC}_2\text{H}_5]_{t=0}} = \frac{\alpha}{1 - \frac{k_{28}}{k_1}} (1-x) [(1-x)^{k_{28}/k_1} - 1] \quad (\text{IV})$$

where α is the yield of product during the chlorine atom initiated oxidation of methyl propionate, k_{28} is the rate constant for reaction 28, and x is the fractional loss of methyl propionate defined as

$$x = 1 - \frac{[\text{C}_2\text{H}_5\text{C}(\text{O})\text{OCH}_3]_t}{[\text{C}_2\text{H}_5\text{C}(\text{O})\text{OCH}_3]_{t=0}} \quad (\text{V})$$



Rate constants obtained from nonlinear least-squares fits of expression IV to the data in Figure 6 are summarized in Table 4. Within the admittedly substantial experimental uncertainties, the results obtained from fitting the shapes of the product yield plots in

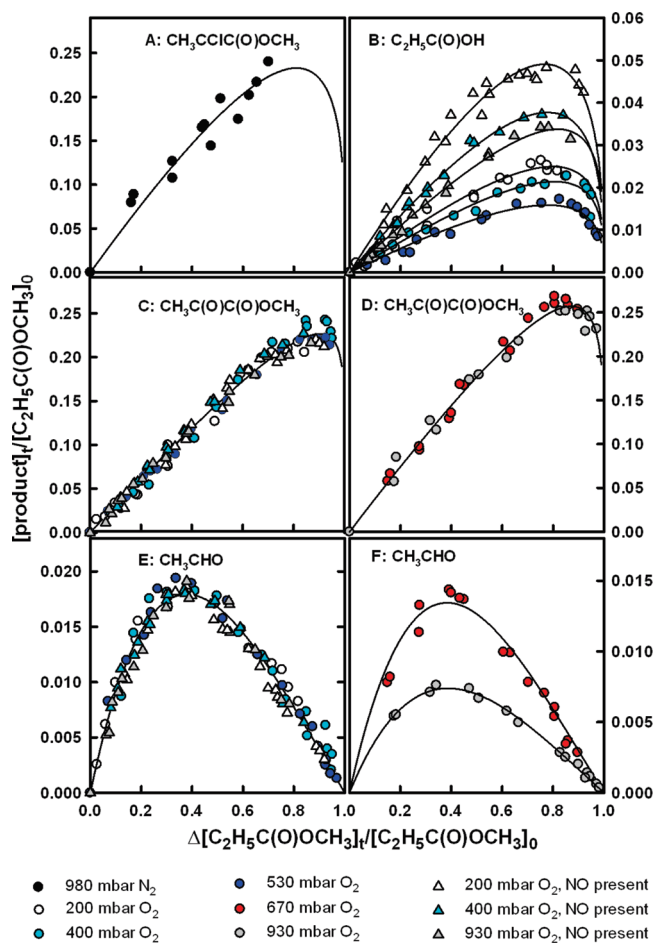


Figure 6. Formation of products versus loss of methyl propionate in 930–980 mbar total pressure of N_2 diluent in the presence (triangles) or absence (circles) of NO with oxygen partial pressures of either 0 mbar (black), 200 mbar (white), 400 mbar (cyan), 530 mbar (blue), 670 mbar (red), or 930 mbar (gray).

Figure 6 are consistent with those reported in the literature or in previous sections of the present paper. The shapes of the product plots in Figure 6 are consistent with the formation and loss of these products initiated by reactions with chlorine atoms.

Molar product yields are shown in Table 5. As indicated in Table 5, for experiments conducted in the absence of NO, small amounts of propionic acid were observed. The yield of propionic acid decreased with increasing oxygen partial pressure. For oxygen partial pressures of 670 mbar and above, no propionic acid (yield <2%) was detected. In the presence of NO, the yields of propionic acid were larger than those obtained for experiments conducted in the absence of NO, but there was still a dependence on oxygen partial pressure. The oxygen dependency reflects a competition between α -ester rearrangement (giving propionic acid) and reaction with oxygen (giving propionic formic anhydride) as fates of $\text{C}_2\text{H}_5\text{C}(\text{O})\text{OCH}_2\text{O}$ alkoxy radicals. Similar behavior was reported by Christensen et al.²⁸ and Tyndall et al.²⁷ for the $\text{CH}_3\text{C}(\text{O})\text{OCH}_2\text{O}$ alkoxy radical formed in the oxidation of methyl acetate. Christensen et al.²⁸ attributed this phenomenon to the formation of chemically activated alkoxy radicals in the reaction of peroxy radicals with NO (reaction 20) which have enough energy to overcome the barrier for α -ester rearrangement²⁸ and

Table 4. Rate Constants for Reactions of Products Formed in the Cl-Initiated Oxidation of Methyl Propionate

reaction	$k \times 10^{12}$ cm ³ molecule ⁻¹ s ⁻¹	reference
CH ₃ CHClC(O)OCH ₃ + Cl → products	4.35 ± 2.02	this study ^a
C ₂ H ₅ C(O)OH + Cl → products	0.695 ± 0.293	this study ^a
C ₂ H ₅ C(O)OH + Cl → products	0.472 ± 0.062	7
CH ₃ C(O)C(O)OCH ₃ + Cl → products	0.303 ± 0.108	this study ^a
CH ₃ CHO + Cl → products	69.8 ± 24.2	this study ^a
CH ₃ CHO + Cl → products	80	39

^aDerived from a fit to the experimental data from the product studies.

decompose on a time scale sufficiently short that reaction with O₂ does not compete. The maximum yield of propionic acid was observed with an oxygen partial pressure of 200 mbar in the presence of NO where the yield is 0.094 ± 0.014. We conclude that at least 9.4 ± 1.4% of the H-abstraction by atomic chlorine from methyl propionate occurs from the -OCH₃ group.

The magnitude of the effect of oxygen partial pressure on the acid yield in the Cl atom initiated oxidation of methyl propionate in the absence of NO observed in the present work is similar to that reported by Christensen et al. for experiments using methyl acetate; both studies observe a decrease in acid yield by a factor of approximately 1.5 on increasing the oxygen partial pressure from 200 to 530 mbar. As seen in Figure 6, for experiments performed in the absence of NO, there was a small, but discernible, influence of [O₂] on the yields of methyl pyruvate and acetaldehyde. As seen by comparing panels C and D in Figure 6, at the highest [O₂] employed the yield of methyl pyruvate was slightly larger than that obtained in experiments using lower [O₂]. The increase in methyl pyruvate comes at the expense of the acetaldehyde yield (compare panels E and F). Interestingly, for experiments performed in the presence of NO there was no discernible influence of [O₂] on the yields of either methyl pyruvate or acetaldehyde and the yields were indistinguishable from those observed in the absence of NO with 200–530 mbar of O₂.

Following Cavalli et al.⁷ we attribute the oxygen dependence to a competition between reactions 23 and 24 for the available CH₃CHOC(O)OCH₃ radicals. Decomposition via reaction 23 gives acetaldehyde and reaction with oxygen gives methyl pyruvate. The combined yields of acetaldehyde and methyl pyruvate provide a marker for reaction of chlorine atoms at the -CH₂- group in methyl propionate. The combined yield of the two compounds at oxygen partial pressures of 200–670 mbar is 0.418 ± 0.042. In the absence of NO in 930 mbar O₂ the combined yield is 0.423 ± 0.051. There is no discernible effect of [O₂] on the combined yields of acetaldehyde and methyl pyruvate. Furthermore, the average combined yield of 0.421 ± 0.067 observed in all the experiments conducted in the presence of O₂ is consistent with the 0.366 ± 0.071 yield of CH₃CHClC(O)OCH₃ in experiments in N₂ diluent. We conclude that 42.1 ± 6.7% of H-abstraction from methyl propionate by atomic chlorine occurs from the secondary α-carbon atom.

The yields of methyl pyruvate, acetaldehyde, and propionic acid in the present study of 0.320 ± 0.046, 0.114 ± 0.021, and 0.094 ± 0.014 in the experiment with 200 mbar partial pressure of oxygen in the presence of NO (see Table 5) can be compared to values of 0.289 ± 0.057, 0.077 ± 0.015, and 0.139 ± 0.019

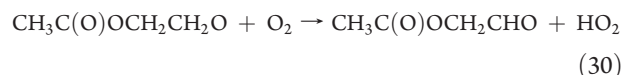
obtained by Cavalli et al. at 740 Torr air in the presence of NO.⁷ Our product yields are generally consistent with those reported previously by Cavalli et al.⁷ although our yield for acetaldehyde is slightly higher and that for propionic acid is slightly lower than that reported by Cavalli et al.⁷ The origin of these small discrepancies is not clear.

6.2. Ethyl Acetate. The products of the chlorine atom initiated oxidation of ethyl acetate were studied using oxygen partial pressures of 70–930 mbar in the presence and absence of NO in 930 mbar total pressure with N₂ diluent. The oxidation mechanism for ethyl acetate is given in Figure 7. In principle, the reaction of chlorine atoms with ethyl acetate will give three different radicals (reactions 4a–4c). However, by analogy to the behavior of methyl acetate¹⁵ we would expect channel 4c to be of negligible importance.



Peroxy and alkoxy radicals are formed from these radicals by reactions similar to those discussed for methyl propionate.

Acetic acid, acetic acid anhydride, acetic formic anhydride, and formaldehyde were identified as products of the chlorine atom initiated oxidation of ethyl acetate in the absence of NO. In the presence of NO, CH₃C(O)OONO₂ (PAN) was also observed. Acetic acid can be formed from the radicals generated by H-abstraction from either of the carbon atoms on the ethyl group (reaction 4a and 4b), via decomposition or rearrangement. The rearrangement and decomposition of the primary alkoxy radical are shown in reactions 29a and 29b. An additional potential fate is reaction with O₂ to give acetoxyacetaldehyde, CH₃C(O)OCH₂CHO (reaction 30). This compound is not commercially available, and its formation could therefore not be confirmed.



The alkyl radical generated in reaction 29b is the same as that formed in the oxidation of methyl acetate. Addition of O₂ followed by reaction with NO gives the alkoxy radical, CH₃C(O)OCH₂O. As discussed in the previous section, there are two competing fates for CH₃C(O)OCH₂O radicals; α-ester rearrangement giving acetic acid and a formyl radical, and reaction with O₂ giving acetic formic anhydride.²⁹



The alkoxy radical generated via H-abstraction from the secondary alkyl carbon in ethyl acetate can undergo α-ester rearrangement to give CH₃C(O)OH and CH₃CO (reaction 33), reaction with oxygen to give acetic acid anhydride (reaction 34), or

In the absence of NO, CH_3O can be formed by self-reaction of methyl peroxy radicals (similar to reaction 21 for methyl propionate).

Figures 8 and 9 show spectra from the product study in air in the absence and presence of NO, respectively. Comparison of the residual spectrum after subtraction of ethyl acetate shown in Figure 8B with the spectra in panels C and D clearly shows the presence of acetic acid and acetic acid anhydride. As seen by comparison of the residual spectrum in Figure 9A with the reference spectrum in panel B, PAN is formed in experiments conducted in the presence of NO_x .

Plots of formation of the observed products versus the loss of ethyl acetate are shown in Figure 10. The formation of acetic acid and acetic acid anhydride correlate linearly with the ethyl acetate loss (see panels A and B). Initially, the increase in formaldehyde correlates linearly with the loss of ethyl acetate. However, chlorine atoms are approximately 4 times more reactive toward formaldehyde than toward ethyl acetate and this leads to the curved product plot in panel E in Figure 10. The curve in panel E is a fit of eq IV, with k_{28} replaced by k_{39} , to the data.



As seen from Figure 10 and Table 6 the yield of formaldehyde is approximately a factor of 3 lower in experiments conducted in the presence of NO than for experiments conducted in the absence of NO. The origins of this difference in the formaldehyde yields are not entirely clear; loss of the CH_3O precursor via reaction with NO_x and a contribution by OH radicals to ethyl acetate oxidation in the presence of NO_x may be contributing factors. The curvature of the plot in panel C of Figure 10 shows that acetic formic anhydride is formed as a secondary product in the absence of NO. The fact that there is little, or no, acetic formic anhydride formed as a primary product indicates that reaction 29b is not important as this decomposition reaction gives $\text{CH}_3\text{C}(\text{O})\text{OCH}_2$ radicals some fraction of which will be converted into acetic formic anhydride via reaction 32. The most probable precursor of acetic formic anhydride is acetoxyacetaldehyde, and thus the approximate yields of 4–8% for acetic formic anhydride give an indication of the minimum yields of acetoxyacetaldehyde.

The yields of acetic acid and acetic acid anhydride were dependent on the oxygen partial pressure, in both the presence and absence of NO. A similar trend for acetic acid anhydride was observed by Orlando and Tyndall in the absence of NO ;¹⁶ we and Orlando and Tyndall observe a decrease by approximately a factor of 1.5 in the yield of acetic acid anhydride over the O_2 partial pressure range of 70 to 930 mbar. The observed product yields are given in Table 6. The yield of acetic acid decreases while that of acetic acid anhydride increases with increasing $[\text{O}_2]$. The combined yield of acetic acid, acetic acid anhydride, and formaldehyde accounts for 91–99% of the ethyl acetate loss for experiments conducted in the absence of NO. The oxygen dependence of the acetic acid and acetic acid anhydride yields is similar to that observed for propionic acid and acetaldehyde in the oxidation of methyl propionate and indicates that there is a competition between α -ester rearrangement and reaction with oxygen as fates for $\text{CH}_3\text{C}(\text{O})\text{OCH}(\text{O})\text{CH}_3$ radicals. It is also possible that there is a competition between reactions 29a and 30, forming more acetic acid at lower oxygen partial pressures. In the present study it was not possible to distinguish between the different reactions leading to the formation of acetic acid, and thus we cannot discern whether the β -rearrangement occurs.

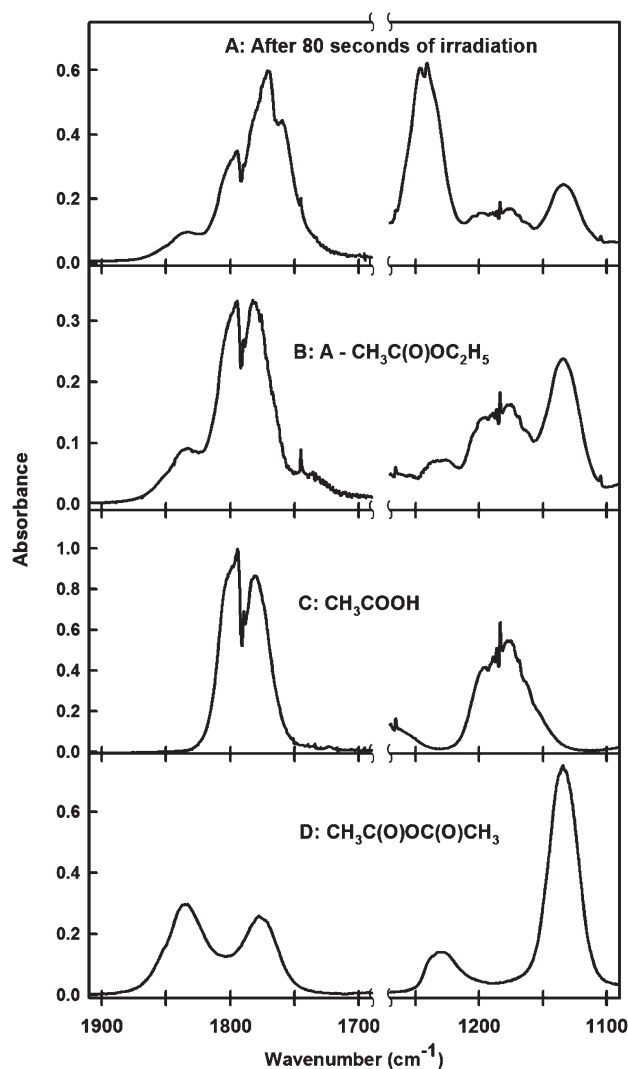


Figure 8. Spectra from the Cl-initiated product study of ethyl acetate in the absence of NO in 930 mbar air. Panel A shows the spectrum after 80 s of UV irradiation. Panel B shows the product spectrum after subtraction of ethyl acetate. Comparison of the spectrum in panel B with those in panels C and D shows the formation of acetic acid and acetic acid anhydride.

Panel C in Figure 10 shows that the secondary formation of acetic formic anhydride (possibly from acetoxyacetaldehyde generated by reaction 30) is also dependent on oxygen partial pressure with a slightly increased yield at higher oxygen partial pressures. This supports the assumption that in the absence of NO acetic formic anhydride is formed from acetoxyacetaldehyde, the formation of which will be oxygen dependent.

The formation of acetic acid anhydride provides a marker for reaction at the secondary alkyl-carbon atom. Thus, the yield at 930 mbar O_2 partial pressure shows that at least $41.2 \pm 6.1\%$ of the reaction of chlorine atoms with ethyl acetate occurs via H-abstraction from the secondary alkyl carbon. The abstraction from this carbon atom is probably significantly higher, as suggested by the substantial yield of acetic acid, however it is not possible to state how much of the acetic acid originates from this route rather than from H-abstraction at the primary alkyl carbon.

PAN formation was observed in the presence of NO_x . This product can be formed from the CH_3CO radical generated by

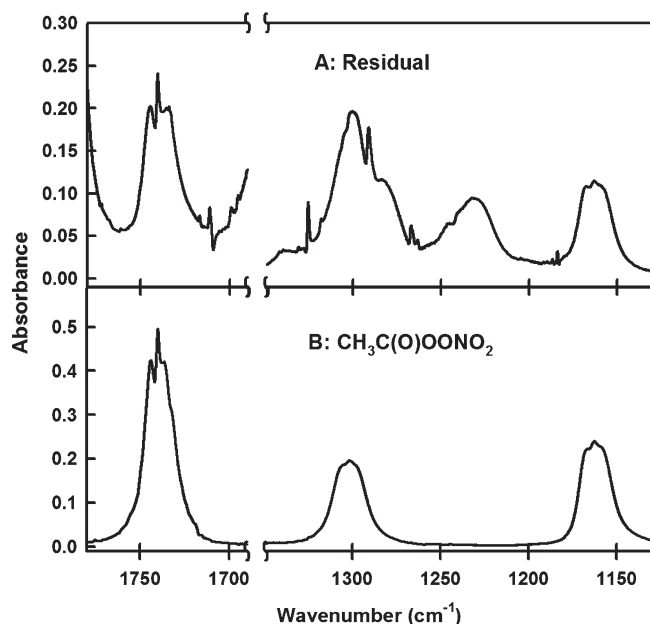
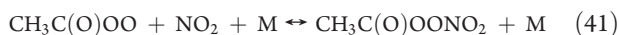
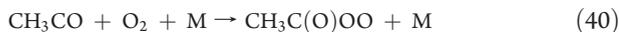


Figure 9. Spectra from the Cl-initiated product study of ethyl acetate in the presence NO in 930 mbar air. Panel A shows the residual spectrum after subtraction of features from ethyl acetate, acetic acid, acetic acid anhydride, acetic formic anhydride, and formaldehyde after 145 s of UV irradiation. Comparison of the residual spectrum with the spectrum in panel B shows the presence of PAN.

reaction 33 via reactions 40 and 41.



The formation of PAN is dependent on the NO/NO₂ ratio, since an additional fate of CH₃C(O)OO is reaction with NO (reaction 42).



For the experiments using [O₂] = 70 mbar and 200 mbar the formation of PAN was observed to be nonlinear (Figure 10, panel F). Initially, when the NO₂ concentration is low, only small amounts of PAN are formed. During the course of the experiment the NO/NO₂ ratio decreases leading to increased formation of PAN. The S-shape of the PAN curves arises from the fact that PAN is thermally unstable and decomposition is an increasingly important factor toward the end of the experiment.¹⁶ At 930 mbar oxygen partial pressure the formation of PAN correlates linearly with the loss of ethyl acetate. At this high oxygen partial pressure a significant fraction of NO was oxidized to NO₂ and thus [NO₂] will be greater than [NO] during the entire course of the experiment. The maximum yields of PAN from ethyl acetate are given in Table 6. At an oxygen partial pressure of 930 mbar the yield of PAN is approximately 70% of the acetic acid yield, and thus it can be concluded that at least 70% of the acetic acid at this oxygen partial pressure is formed by the α-ester rearrangement of the CH₃C(O)OCH(O)CH₃ radical (reaction 33).

The yield of acetic acid was higher, and the yields of acetic acid anhydride and formaldehyde were lower, in the presence of NO. The fact that acetic formic anhydride is only observed as a primary product in the presence of NO suggests that chemical activation plays a role in the fate of CH₃C(O)OCH₂CH₂O

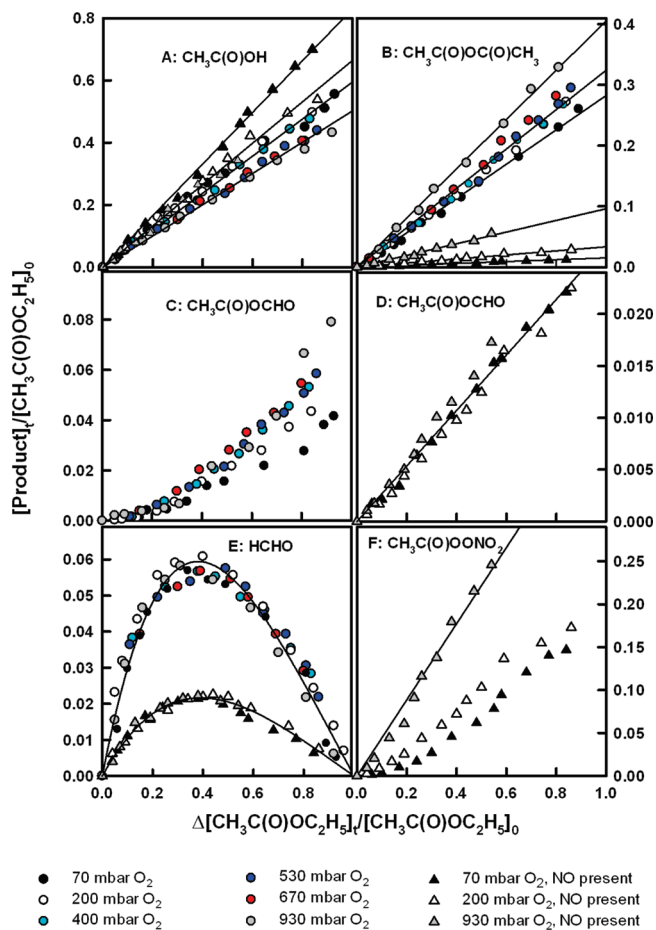


Figure 10. Formation of products versus loss of ethyl acetate in the presence (triangles) and absence (circles) of NO in 930 mbar total pressure of N₂ diluent at the following oxygen partial pressures: 70 mbar (black symbols), 200 mbar (white symbols), 400 mbar (cyan symbols), 530 mbar (blue symbols), 670 mbar (red symbols), and 930 mbar (gray symbols).

and/or CH₃C(O)OCH(O)CH₃ alkoxy radicals. The increased yield of acetic acid in the presence of NO probably reflects participation of OH radicals in the initiation of the oxidation of ethyl acetate. Hydroxyl radicals will be formed in the reaction of HO₂ radicals with NO and Tuazon et al.¹⁴ and Picquet-Varrault et al.¹⁵ have shown that the OH initiated oxidation of ethyl acetate gives acetic acid in a yield of 75–95%.

The present study shows that the reactivity of chlorine atoms toward the secondary alkyl carbon atom is higher than that of the primary alkyl carbon atom. Tuazon et al.¹⁴ and Picquet-Varrault et al.¹⁵ have shown that the same is true for reaction with OH radicals. In our chlorine initiated experiments in the absence of NO_x we observe a substantial yield of acetic acid anhydride. The yield of this product drops dramatically in the presence of NO_x suggesting that its formation in the absence of NO_x is probably attributable to the molecular channel of the self- and cross reactions of CH₃C(O)OCH(O)CH₃ peroxy radicals in the system. The small yield of acetic acid anhydride that we observe in experiments at lower [O₂] in the presence of NO_x is consistent with the report by Picquet-Varrault et al.¹⁵ of a 2 ± 1% yield for this compound in 1 atm of air in the presence of NO_x. We observe acetic formic anhydride as a secondary product in the absence of NO_x which confirms the presence of

Table 6. Product Yields in the Chlorine Atom Initiated Oxidation of Ethyl Acetate in 930-980 mbar Total Pressure of N₂ Diluent^a

product	O ₂ partial pressure (mbar)					
	70	200	400	530	670	930
Molar Yields in % in the Absence of NO						
CH ₃ C(O)OH	57.5 ± 9.5	57.9 ± 7.7	57.5 ± 8.2	50.4 ± 7.7	50.6 ± 7.4	46.7 ± 6.9
CH ₃ C(O)OC(O)CH ₃	28.5 ± 4.5	31.2 ± 4.5	31.6 ± 5.1	32.8 ± 5.9	34.5 ± 6.3	41.2 ± 6.1
HCHO	34.7 ± 7.4	38.1 ± 6.2	34.0 ± 8.9	33.0 ± 7.9	31.9 ± 5.7	35.7 ± 7.8
Molar Yields in % in the Presence of NO						
CH ₃ C(O)OH	84.6 ± 11.9	65.8 ± 10.1				64.8 ± 10.7
CH ₃ C(O)OC(O)CH ₃	1.5 ± 0.2	3.4 ± 0.6				10.2 ± 1.7
CH ₃ C(O)OCHO	2.7 ± 0.4	2.6 ± 0.4				3.2 ± 0.5
HCHO	14.3 ± 2.2	11.7 ± 2.1				13.0 ± 2.1
CH ₃ C(O)OONO ₂	18.2 ± 2.9	23.2 ± 2.6				44.9 ± 8.0

^aQuoted errors include 2 standard deviations of fits to the data in Figure 10 and 10% potential systematic uncertainty associated with the IR analysis.

acetoxyacetaldehyde, which was also observed by Picquet-Varrault et al.¹⁵ in the OH-initiated oxidation of ethyl acetate in 1 atm of air and in the presence of NO_x.

We observe an increase in the acetic acid anhydride yield with increasing [O₂] in experiments with NO_x suggesting that there is a competition between reaction with O₂ and α-ester rearrangement as fates of the CH₃C(O)OCH(O)CH₃ alkoxy radical. In experiments without NO_x the increase in acetic acid anhydride is most pronounced at high oxygen partial pressures. Orlando and Tyndall also observed an increase in acetic acid anhydride with increasing oxygen partial pressures.¹⁶ In their study the combined yield of acetic acid and acetic acid anhydride was assumed to stem exclusively from the H-abstraction from the secondary alkyl carbon atom. The combined yields of the two compounds in the study by Orlando and Tyndall (79 ± 5%) is comparable to that observed in the present study (86.7 ± 3.9%) at all oxygen partial pressures in the absence of NO_x at 298 K. Although the individual yields of the two compounds are not significantly different between the two studies, we observe slightly higher yields of acetic acid anhydride and slightly lower yields of acetic acid at all oxygen partial pressures than those reported by Orlando and Tyndall.

7. RESULTS OF COMPUTATIONAL STUDIES

The reaction mechanism for hydrogen abstraction from methyl propionate and ethyl acetate by the hydroxyl radical was investigated theoretically. The OH radical abstracts a hydrogen atom from the –CH₂– or the –CH₃ group; furthermore, the OH radical can abstract either the in-plane or the out-of-plane hydrogen atom on either of the two methyl groups. The in-plane hydrogen atom is less favorable toward abstraction than the out-of-plane.¹⁹ Here we will only consider the hydrogen abstraction of the out-of-plane hydrogen atom of the methyl group.

In Figure 11 the transition states for H-abstraction by the three pathways are shown for methyl propionate and ethyl acetate. Details for the optimized geometries and transition state energies are provided in Tables S3–S5 in the Supporting Information. When the OH radical abstracts a hydrogen atom from one of the two methyl groups in methyl propionate, a hydrogen bond is formed between the hydrogen atom in the hydroxyl radical and the oxygen atom in the carbonyl group (>C=O). The lengths of

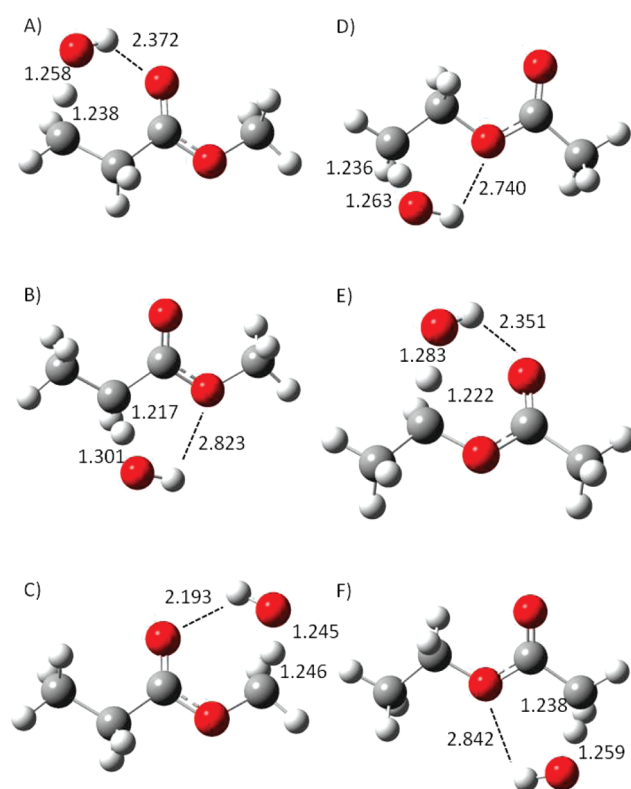


Figure 11. Transition state structures of the following reaction paths: (A) CH₃CH₂C(O)OCH₃ + OH → CH₂CH₂C(O)OCH₃ + H₂O; (B) CH₃CH₂C(O)OCH₃ + OH → CH₃CHC(O)OCH₃ + H₂O; (C) CH₃CH₂C(O)OCH₃ + OH → CH₃CH₂C(O)OCH₂ + H₂O; (D) CH₃C(O)OCH₂CH₃ + OH → CH₃C(O)OCH₂CH₂ + H₂O; (E) CH₃C(O)OCH₂CH₃ + OH → CH₃C(O)OCHCH₃ + H₂O; (F) CH₃C(O)OCH₂CH₃ + OH → CH₂C(O)OCH₂CH₃ + H₂O. The geometries were optimized at BHandHLYP/aug-cc-pVTZ level of theory. Distances are in units of angstroms.

the hydrogen bonds are 2.4 and 2.2 Å for the methyl group in the propionate (Figure 11A) and the methoxy group (Figure 11C), respectively. If the OH radical abstracts one of the hydrogen atoms on the –CH₂– group, there is only a very weak interaction between the hydrogen atom on the hydroxyl group and the

Table 7. Computed Branching Ratios for Reaction of OH with Methyl Propionate and Ethyl Acetate

	branching ratio (%)
methyl propionate	
$\text{CH}_3\text{CH}_2\text{C}(\text{O})\text{OCH}_3 + \text{OH} \rightarrow \text{CH}_2\text{CH}_2\text{C}(\text{O})\text{OCH}_3 + \text{H}_2\text{O}$	34
$\text{CH}_3\text{CH}_2\text{C}(\text{O})\text{OCH}_3 + \text{OH} \rightarrow \text{CH}_3\text{CHC}(\text{O})\text{OCH}_3 + \text{H}_2\text{O}$	43
$\text{CH}_3\text{CH}_2\text{C}(\text{O})\text{OCH}_3 + \text{OH} \rightarrow \text{CH}_3\text{CH}_2\text{C}(\text{O})\text{OCH}_2 + \text{H}_2\text{O}$	23
ethyl acetate	
$\text{CH}_3\text{C}(\text{O})\text{OCH}_2\text{CH}_3 + \text{OH} \rightarrow \text{CH}_2\text{C}(\text{O})\text{OCH}_2\text{CH}_3 + \text{H}_2\text{O}$	0
$\text{CH}_3\text{C}(\text{O})\text{OCH}_2\text{CH}_3 + \text{OH} \rightarrow \text{CH}_3\text{C}(\text{O})\text{OCHCH}_3 + \text{H}_2\text{O}$	99
$\text{CH}_3\text{C}(\text{O})\text{OCH}_2\text{CH}_3 + \text{OH} \rightarrow \text{CH}_3\text{C}(\text{O})\text{OCH}_2\text{CH}_2 + \text{H}_2\text{O}$	1

ether linkage (i.e., $-\text{O}-$); the distance is 2.8 Å (Figure 11B). The opposite trend is observed for ethyl acetate where we observe a hydrogen bond between the hydroxyl radical and the carbonyl group when hydrogen atoms are abstracted from the $-\text{CH}_2-$ group (Figure 11E), whereas a weak interaction between the hydroxyl radical and the ether linkage is observed for hydrogen abstraction on the two methyl groups (panels D and F of Figure 11). We conclude that stabilization of the transition state for H-abstraction from the $-\text{CH}_2-$ group depends on the surrounding group. The carbonyl group is more effective than an ether linkage at stabilizing the transition state for abstraction from a $-\text{CH}_2-$ group. The $-\text{CH}_2-$ group in ethyl acetate is activated, whereas in methyl propionate it is deactivated.

We have estimated the rates of H-abstraction for each of the hydrogen atoms. The total rate is the sum of the individual rate constants. The overall rate constant is estimated at 298 K and 1 atm. The computed rate constants are given in Table 1. We underestimate the rate constant for methyl propionate whereas we overestimate the rate constant for ethyl acetate. The branching ratio is the ratio between the individual rates and the total rate. The branching ratios for methyl propionate and ethyl acetate are given in Table 7. In the case of methyl propionate approximately 43% of the reaction occurs at the $-\text{CH}_2-$ group, whereas for ethyl acetate essentially all ($\sim 99\%$) of the reaction occurs at the $-\text{CH}_2-$ group.

With the structure activity relationship (SAR) method outlined by Kwok and Atkinson³³ with $F(-\text{CH}_2\text{C}(\text{O})\text{OR}) = 2.2$ from Le Calvé et al.³⁴ it can be estimated that attack of OH radicals occurs 25%, 57%, and 18% at the CH_3- , $-\text{CH}_2-$, and $-\text{OCH}_3$ groups in methyl propionate. Similarly with values of $F(-\text{OC}(\text{O})\text{R}) = 1.6$ and $F(-\text{C}(\text{O})\text{OR}) = 0.74$, it can be estimated that attack of OH radicals on ethyl acetate occurs 9%, 85%, and 6% at the CH_3- , $-\text{CH}_2-$, and $-\text{C}(\text{O})\text{CH}_3$ in ethyl acetate. Our theoretically determined branching ratios given in Table 7 are broadly consistent, within the combined expected uncertainties inherent in such calculations with the values estimated using SAR methods. We note that the calculation of branching ratios is more accurate and converges more quickly than the calculation of absolute rate constants. The dominance of abstraction from the $-\text{CH}_2-$ group in ethyl acetate indicated from the ab initio calculations is consistent with the observation of acetic acid product in a yield of 75–95% reported in the experimental studies by Tuazon et al.¹⁴ and Picquet-Varrault et al.¹⁵

8. IMPLICATIONS FOR ATMOSPHERIC CHEMISTRY

The present work serves to confirm and refine our understanding of the kinetics of the reactions of chlorine atoms and OH radicals with methyl propionate and ethyl acetate. We report the first ab initio studies of the mechanisms of the reactions of the reactions of OH radicals with methyl propionate and ethyl acetate. The results from the ab initio studies are consistent with results from previously reported experimental product studies of ethyl acetate oxidation and SAR calculations of the reaction of OH with methyl propionate. The atmospheric oxidation of esters is initiated by reaction with hydroxyl radicals. Atmospheric lifetimes of the esters can therefore be estimated from their reaction rates with the hydroxyl radical. The rate constants determined in this study together with a global average OH concentration of $1 \times 10^6 \text{ cm}^{-3}$ ³⁵ give lifetimes of approximately 8 and 12 days for ethyl acetate and methyl propionate. As indicated from the linearity of most of the product plots in Figures 6 and 10, the degradation products of methyl propionate and ethyl acetate tend to be less reactive than the parent esters. Given their modest kinetic and mechanistic reactivity, it is expected that methyl propionate and ethyl acetate are relatively inefficient in contributing to local air quality impacts. This expectation is borne out by the modest photochemical ozone creation potential estimated by Saunders et al.³⁶ for ethyl acetate.

As with all other classes of organic compounds, the reactivity of esters toward OH radicals will increase with the size of the ester reflecting the increased number of reactive sites in the molecule. As shown in the present study the effect is more pronounced for increased size of the alkoxy rather than the acyl end of the molecule (ethyl acetate is more reactive than methyl propionate). Biodiesel typically contains methyl esters of long chain fatty acids (e.g., methyl palmate, $\text{CH}_3(\text{CH}_2)_{14}\text{C}(\text{O})\text{OCH}_3$; methyl stearate, $\text{CH}_3(\text{CH}_2)_{16}\text{C}(\text{O})\text{OCH}_3$). The atmospheric reactivity of the long chain fatty acid methyl esters is expected to approach that of the corresponding alkanes as the chain length increases and the ester functionality exercises less influence on the overall chemistry of the molecule. Further experimental and computational studies of the atmospheric chemistry of larger esters more representative of biodiesel would be helpful in better elucidating the atmospheric fate of these molecules.

■ ASSOCIATED CONTENT

S Supporting Information. Experimental conditions and results for relative rate studies of the Cl and OH initiated oxidations of methyl propionate, methyl-2-chloropropionate, and ethyl acetate (Table S1), experimental conditions for product studies of the Cl initiated oxidations of methyl propionate and ethyl acetate (Table S2), the electronic energies (E) and the zero point vibrational energies (ZPE) of the reactants and the transition states (Table S3), the rotational constants (in GHz) and the vibrational frequencies (in cm^{-1}) for the BHandHLYP/aVTZ geometries (Table S4), the coordinate for the optimized structures of methyl propionate, ethyl acetate, hydroxyl radical, and transition state structures (Table S5), and absorption cross sections of methyl propionate and ethyl acetate (Figure S1). This information is available free of charge via the Internet at <http://pubs.acs.org>.

■ AUTHOR INFORMATION

Corresponding Author

*E-mail: msj@kiku.dk.

ACKNOWLEDGMENT

The authors thank the Copenhagen Center for Atmospheric Research, sponsored by the Danish Natural Science Research Council, the Villum Kann Rasmussen Fund, and EURO-CHAMP2, for its generous support.

REFERENCES

- (1) Bendtz, K. *EU-25 - Oilseeds and products: Biofuels situation in the European Union 2005, GAIN report*; USDA and Foreign Agricultural Service: Washington DC, 2007.
- (2) Worldwatch Institute *Biofuels for transport*. London: Earthscan: Oxford, 2007.
- (3) European Biodiesel Board. <http://www.ebb-eu.org/stats.php>, 2010
- (4) Mellouki, A.; Le Bras, G.; Sidebottom, H. *Chem. Rev.* **2003**, *103*, 5077.
- (5) Calvert, J. G.; Mellouki, A.; Orlando, J. J.; Pilling, M. J.; Wallington, T. J., *Mechanisms of Atmospheric Oxidation of the Oxygenates*; Oxford University Press: Oxford and New York, 2011.
- (6) Notario, A.; Le Bras, G.; Mellouki, A. *J. Phys. Chem. A* **1998**, *102*, 3112.
- (7) Cavalli, F.; Barnes, I.; Becker, K. H.; Wallington, T. J. *J. Phys. Chem. A* **2000**, *104*, 11310.
- (8) Wallington, T. J.; Dagaut, P.; Liu, R.; Kurylo, M. J. *Int. J. Chem. Kinet.* **1988**, *20*, 177.
- (9) Le Calvé, S.; Le Bras, G.; Mellouki, A. *J. Phys. Chem. A* **1997**, *101*, 9137.
- (10) Cuevas, C. A.; Notario, A.; Martinez, E.; Albaladejo, J. *Atmos. Environ.* **2005**, *39*, 5091.
- (11) Xing, J.-H.; Takahashi, K.; Hurley, M. D.; Wallington, T. J. *Chem. Phys. Lett.* **2009**, *474*, 268.
- (12) El Boudali, A.; Le Calvé, S.; Le Bras, G.; Mellouki, A. *J. Phys. Chem.* **1996**, *100*, 12364.
- (13) Picquet-Varrault, B.; Heroux, S.; Chebbi, A.; Doussin, J.-F.; Durand-Jolibois, R.; Monod, A.; Loirat, H.; Carlier, P. *Int. J. Chem. Kinet.* **1998**, *30*, 839.
- (14) Tuazon, E. C.; Aschmann, S. M.; Atkinson, R.; Carter, W. P. L. *J. Phys. Chem. A* **1998**, *102*, 2316.
- (15) Picquet-Varrault, B.; Doussin, J.-F.; Durand-Jolibois, R.; Carlier, P. *Phys. Chem. Chem. Phys.* **2001**, *3*, 2595.
- (16) Orlando, J. J.; Tyndall, G. S. *Int. J. Chem. Kinet.* **2010**, *42*, 397.
- (17) Nilsson, E. J.; Eskebjerg, C.; Johnson, M. S. *Atmos. Environ.* **2009**, *43*, 3029.
- (18) Wallington, T. J.; Gierczak, C. A.; Ball, J. C.; Japar, S. M. *Int. J. Chem. Kinet.* **1989**, *21*, 1077.
- (19) Jørgensen, S.; Andersen, V. F.; Nilsson, E. J. K.; Nielsen, O. J.; Johnson, M. S. *Chem. Phys. Lett.* **2010**, *490*, 116.
- (20) Lee, C. T.; Yang, W. T.; Parr, R. G. *Phys. Rev. B* **1998**, *37*, 785.
- (21) Becke, A. D. *J. Chem. Phys.* **1993**, *98*, 1372.
- (22) Dunning, T. H. *J. Chem. Phys.* **1989**, *90*, 1007.
- (23) Pople, J. A.; Head-Gordon, M.; Raghavachari, K. *J. Chem. Phys.* **1987**, *87*, 5968–5975.
- (24) Frisch, M. J. et al. *GAUSSIAN 03, Revision C.02*; GAUSSIAN, Inc.: Wallingford, CT, 2004.
- (25) McQuarrie, D. A. *Statistical Mechanics*; Harper Collins Publisher: New York, 1976.
- (26) Wigner, E. Z. *Phys. Chem., Abt. B* **1932**, *19*, 203–216.
- (27) Tyndall, G. S.; Pimentel, A. S.; Orlando, J. J. *J. Phys. Chem. A* **2004**, *108*, 6850.
- (28) Christensen, L. K.; Ball, J. C.; Wallington, T. J. *J. Phys. Chem. A* **2000**, *104*, 345.
- (29) Andersen, V. F.; Nilsson, E. J. K.; Jørgensen, S.; Nielsen, O. J.; Johnson, M. S. *Chem. Phys. Lett.* **2009**, *472*, 23.
- (30) Nilsson, E.; Johnson, M. S.; Taketani, F.; Matsumi, Y.; Hurley, M. D.; Wallington, T. J. *Atmos. Chem. Phys.* **2007**, *7*, 5873.
- (31) Christensen, L. K.; Wallington, T. J.; Gushin, A.; Hurley, M. D. *J. Phys. Chem. A* **1999**, *103*, 4202.
- (32) Meagher, R. J.; McIntosh, M. E.; Hurley, M. D.; Wallington, T. J. *Int. J. Chem. Kinet.* **1997**, *29*, 619.
- (33) Kwok, E. S. C.; Atkinson, R. *Atmos. Environ.* **1995**, *29*, 1685.
- (34) Le Calvé, S.; Le Bras, G.; Mellouki, A. *J. Phys. Chem. A* **1997**, *101*, 9137.
- (35) Prinn, R.; Weiss, R. F.; Miller, B. R.; Huang, J. A.; Cunnold, D. M.; Fraser, P. J.; Hartley, D. E.; Simmonds, P. G. *Science* **1995**, *269*, 187.
- (36) Saunders, S. M.; Jenkin, M. E.; Derwent, R. G.; Pilling, M. J. *Atmos. Chem. Phys.* **2003**, *3*, 161.
- (37) Wine, P. H.; Semmes, D. H. *J. Phys. Chem.* **1983**, *87*, 3572.
- (38) Wallington, T. J.; Andino, J. M.; Lorkovic, I. M.; Kaiser, E. W.; Marston, G. *J. Phys. Chem.* **1990**, *94*, 3644.
- (39) Atkinson, R.; Baulch, D. L.; Cox, R. A.; Crowley, J. N.; Hampson, R. F.; Hynes, R. G.; Jenkin, M. E.; Rossi, M. J.; Troe, J. *Atmos. Chem. Phys.* **2006**, *6*, 3625.
- (40) Calvert, J. G.; Derwent, R. G.; Orlando, J. J.; Tyndall, G. S.; Wallington, T. J. *Mechanism of atmospheric oxidation of the alkanes*; Oxford University Press: Oxford and New York, 2008.